Dalton Transactions

One-dimensional DABCO hydrogen-bonding chain in a hexagonal channel of magnetic $[Ni(dmit)_2]$

Journal:	*Dalton Transactions*
Manuscript ID	DT-ART-09-2020-003386.R2
Article Type:	Paper
Date Submitted by the Author:	04-Nov-2020
Complete List of Authors:	Li, Simin; Hokkaido University, Graduate School of Environmental Science Takahashi, Kiyonori; Hokkaido University, Research Institute for Electronic Science; Hokkaido University, Graduate School of Environmental Science Hisaki, Ichiro; Osaka University Graduate School of Engineering Science School of Engineering Science, Research Institute for Electronic Science Kokado, Kenta; Hokkaido University, Research Institute for Electronic Science Nakamura, Takayoshi; Hokkaido University, Research Institute for Electronic Science

ARTICLE

One-dimensional DABCO hydrogen-bonding chain in a hexagonal channel of magnetic [Ni(dmit)$_2$]

Received 00th January 20xx,
Accepted 00th January 20xx

DOI: 10.1039/x0xx00000x

Simin Li,[a] Kiyonori Takahashi,*[a,b] Ichiro Hisaki,[c] Kenta Kokado, [a,b,d] Takayoshi Nakamura*[a,b]

Crystals of (HDABCO$^+$)$_9$(DABCO)[Ni(dmit)$_2$]$_9$•6CH$_3$CN were shown to have a space group of *R*-3, a hexapetal flower-like channel of [Ni(dmit)$_2$] anions, and a one-dimensional hydrogen bonding chain composed of protonated DABCO and CH$_3$CN molecules. The crystals display antiferromagnetic and ferromagnetic interactions within and between hexamers, respectively, whereas the flexible DABCO-CH$_3$CN array shows dielectric relaxation.

Introduction

Molecules possessing multiple hydrogen bonding sites often have unique dielectric properties in their crystalline states,[1–7] and as a result, they are promising ferroelectric candidates.[7–16] Rearrangements of hydrogen bonds between proton donating and accepting sites is the origin of the dielectric responses of these substances. Examples of substances of this type are squaric and croconic acid, whose molecules in the crystalline state form two dimensional sheet structures through O-H•••O hydrogen bonding interactions between hydroxyl hydrogens and carbonyl oxygens.[1,7] The collective proton transfers result in large dielectric responses in the disordered state of squaric acid[1,2] and a ferroelectric transition in croconic acid with a spontaneous polarization of 21 μC cm^{-2}.[7]

Besides O-H•••O hydrogen bonding networks, those involving nitrogen as the proton acceptor (eg., N-H$^+$•••N) have been utilized for constructing interesting dielectric substances. Of particular interest in this regard are 1,4-diazabicyclo[2.2.2]octane (DABCO) and its derivatives,[17–19] which contain nitrogen atoms locate at axial positions of cylindrically shaped structures and whose mono protonated salts in their crystalline states often form one-dimensional chains through N-H$^+$•••N bonds. The one-dimensional polycationic chains that exist in HDABCO$^+$Br$^-$ crystals exhibit very large dielectric responses along the hydrogen bonding direction, which originate from a short-range polar order as a consequence of weak proton correlations.[20] Similar dielectric responses have been observed for ClO_4^-, BF_4^- , and ReO_4^- salts of HDABCO$^+$.[9,21]

The crystal of (HDABCO$^+$)$_2$(TCNQ)$_3$ (TCNQ = 7,7,8,8-tetracyano-*p*-quinodimethane) undergoes a ferroelectric transition caused by concerted proton transfer within one-dimensional dielectric (N•••H•••N)$_\infty$ hydrogen-bonding chains.[22] This transition displays a large deuterium isotope effect.[22] In general, molecular assemblies of open-shell π-electron systems in ion-radical states provides conduction carriers and have magnetic spins, although TCNQ anion radicals in (HDABCO$^+$)$_2$(TCNQ)$_3$ formed a strong trimer unit with two *S* = 1/2 spins in the singlet state.

As part of our interest in exploring the magnetic properties of substances in which unique electronic systems are coupled with dielectric hydrogen-bonding networks, our attention became focused on the [Ni(dmit)$_2$] (dmit^{2-} = 2-thioxo-1,3-dithiole-4,5-dithiolate) complex, which is planar and has an open shell electronic structure.[23,24] The SOMO of [Ni(dmit)$_2$] is composed of a π-orbital array with a node (small single electron density) at Ni atom.[25] Therefore, [Ni(dmit)$_2$] is an excellent building block for constructing π-electron systems possessing conduction electrons and/or magnetic spins. In the investigation described below, we prepared a crystal of (HDABCO$^+$)$_9$(DABCO)[Ni(dmit)$_2$]$_9$•6CH$_3$CN (**1**) and found that it has a highly symmetric structure, in which [Ni(dmit)$_2$] anions are part of a hexapetal flower-like pattern with the one-dimensional chains of DABCO and CH$_3$CN located at the center. In this paper, we describe intriguing structure of the crystal in detail together with dielectric and magnetic properties.

Experimental

General

All reagents were used without further purification. Elemental analyses were carried out by using a CHN analyzer (CE440, Exeter Analytical, Inc.) at the Instrumental Analysis Division, Equipped Management Center, Creative Research Institution, Hokkaido University.

[a] *Graduate School of Environmental Science, Hokkaido University, N10W5, Kita-ku, Sapporo 060-0810, Japan*
[b] *Research Institute for Electronic Science (RIES), Hokkaido University, N20W10, Kita-ku, Sapporo, 001-0020, Japan*
[c] *Graduate School of Engineering Science, Osaka University, 1-3, Machikaneyama, Toyonaka, Osaka, 560-0043, Japan*
[d] *JST-PRESTO, Honcho 4–1-8, Kawaguchi, Saitama 332-0012, Japan.*
E-mail: (KT) ktakahashi@es.hokudai.ac.jp, (TN) tnaka@es.hokudai.ac.jp
Electronic Supplementary Information (ESI) available: See DOI: 10.1039/x0xx00000x

Crystal Preparation

Precursors of (tetra-*n*-butylammonium)[Ni(dmit)$_2$] and (HDABCO$^+$)(BF$_4^-$) were prepared using literature described methods.[9,26] Single crystals of (HDABCO$^+$)$_9$(DABCO)[Ni(dmit)$_2$]$_9$•6CH$_3$CN (**1**) were prepared by using an evaporation method at 50 degree. The green solution of (tetra-*n*-butylammonium)[Ni(dmit)$_2$] (104 mg) in acetone (50 mL) was slowly added to a colorless solution of (HDABCO$^+$)(BF$_4^-$) (60 mg) in CH$_3$CN (50 mL). After several days, single crystals were obtained as black thin plates (yield: 74 mg, 82 %). Anal. Calcd (%) for $C_{126}H_{147}N_{26}Ni_9S_{90}$ (5439.78): C,27.82; H, 2.72 N, 6.69. Found: C, 27.54; H, 2.54; N, 6.37.

Crystal Structure Determination

Temperature-dependent x-ray crystallographic analysis of single crystals of **1** was performed using a Rigaku MicroMax-007HF diffractometer with a Pilatus 200 K detector and $Cu_{K\alpha}$ radiation (λ = 1.54184 Å). Multi-scan absorption corrections were applied to the reflection data. A single crystal was mounted on MicroMounts™ tip (MiTeGen) with Paratone® 8277 (Hampton Research). The temperature dependence was measured on the same crystal. Data collection, cell refinement, and data reduction were carried out with Crysalis^{PRO} (Rigaku Oxford Diffraction, 2017). The initial structure was solved by using SHELXT,[27] and structural refinement was performed by using full-matrix least-squares techniques on F^2 using OLEX2 package.[28] Anisotropic refinement was applied to all atoms except for hydrogens. These data are provided free of charge in The Cambridge Crystallographic Data Centre (CCDC No. 2025004, 2025002, and 2025003 for crystal **1** at 123, 173, and 223 K, respectively).

Magnetic Measurements

Temperature-dependent magnetic susceptibilities were measured with a Quantum Design MPMS3 SQUID magnetometer. A magnetic field of 1 T was applied for all temperature-dependent measurements. Prior to each determination, a measurement was made on the sample holder (plastic wrap) under identical conditions and then directly subtracted from the obtained data as the diamagnetic contribution. Diamagnetic constants based on Pascal's law (-2.69706×10^{-3} cm^{3}mol^{-1}) were also subtracted from the obtained magnetic susceptibility.[29]

Dielectric Measurement

Temperature and frequency dependent dielectric constant (ε_1) and tangent delta (tan(δ)) were measured using an Agilent 4294A with two-probe AC impedance method at a frequency range from $10^{2.5}$ to 10^6 Hz with $10^{0.5}$ Hz increment. Electrical contacts were prepared using gold paste to attach the 10 μm ϕ gold wires to the crystals. Measurements were carried out along the *c* axis. Temperature was controlled in a cryogenic refrigeration system (JECC TORISHA Co., Ltd) with a temperature controller model 330 (Lake Shore Cryotronics Inc.).

Calculation of Transfer Integrals

The extended Hückel molecular orbital method within the tight-binding approximation was applied to calculate the transfer integrals (*t*) between [Ni(dmit)$_2$] anions. The lowest-unoccupied molecular orbital of the [Ni(dmit)$_2$] molecule was used as the basis function.[30] According to the literature, semiempirical parameters for Slater-type atomic orbitals were obtained.[30] The *t* values between each pair of molecules were assumed to be proportional to the overlap integral (*S*) according to the equation $t = -10\,S$ eV.

TG-DTA

Thermogravimetric analysis was conducted using a Rigaku Thermo Plus TG8120 with a heating rate of 10 K/min under nitrogen gas flow.

Results and discussion

Synthesis

The preparation of (HDABCO$^+$)$_9$(DABCO)[Ni(dmit)$_2$]$_9$•6CH$_3$CN (**1**) was achieved by using a cation exchange reaction of (tetra-*n*-butylammonium$^+$)[Ni(dmit)$_2$] with HDABCO$^+$, which leads to formation of a variety of polymorphs and pseudo polymorphs. By using a mixture of acetone and acetonitrile for this process, we obtained single crystals of one polymorph of **1**, whose composition was determined by using elemental and X-ray analyses. Assignment of the number of CH$_3$CN molecules in **1** was also confirmed by employing thermogravimentric (TG) measurements (Fig. S1).

Crystal structure

Inspection of the crystal structure of **1** at 173 K, displayed in Fig. 1 shows that it belongs to the highly symmetric space group of *R*-3 of trigonal crystal system. Ten thirds of DABCO molecules, three [Ni(dmit)$_2$] anions, and two acetonitrile molecules comprise a crystallographically independent asymmetric unit (Fig. S4) In the crystals of **1**, [Ni(dmit)$_2$] anions form a hexapetal flower-like structure and the channels that exist between the honeycomb distribution of [Ni(dmit)$_2$] anions are filled with one-dimensional chains composed of DABCO and CH$_3$CN molecules. Radical ions have a strong tendency to form dimers as well as columnar structures in the crystal state through π-π interactions, which prevents hexagonal arrangements as seen in the crystal **1**. In addition, hexagonal molecular arrangements of π-ion radicals are rare. One example is the conducting crystal of (DIPS)$_3$PF$_6$(chlorobenzene)$_{1.15}$ (DIPS = diiodo(pyrazino)diselenadithiafulvalene), in which DIPS formed a planer hexamer constructed through I•••N interactions surrounding PF$_6$ anion.[31] Planer hexamers stacked one-dimensionally giving relatively high conductivity through π-π interaction. Crystal of [TTF$^+$]$_2$[C$_6$(COO)$_6$H$_4^{2-}$] (TTF = tetrathiafulvalene) has the space group of $P6_422$.[32] However, only the deprotonated benzene hexacarboxylic acid molecules formed a hexagonal channel in the crystal, while the TTF cation radicals formed a one-dimensional columnar structure within the [C$_6$(COO)$_6$H$_4^{2-}$] channel. In both cases, strong interaction between ion radicals resulted in one-dimensional π-stack showing keen difference from present crystal in which edge-on assembly of [Ni(dmit)$_2$] anions surround one-dimensional DABCO-CH$_3$CN chains (Fig 1(b)).

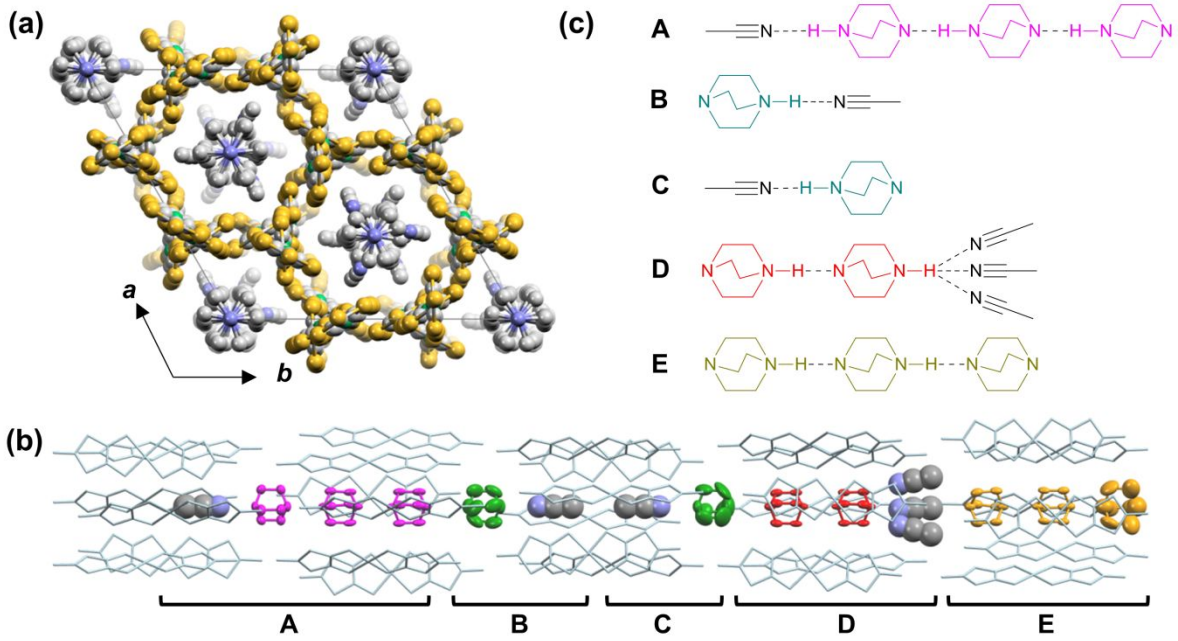

Fig. 1 (a) Ball and stick stick model of the packing structure of $(HDABCO^+)_9(DABCO)[Ni(dmit)_2]_9 \bullet 6CH_3CN$ (**1**) viewed along the *c* axis. C, N, O, S and Ni atoms are depicted in gray, blue, red, yellow, and green, respectively. (b) One-dimensional DABCO-CH_3CN arrays in a unit cell. One chain **A-B-C-D-E-E'-D'-C'-B'-A'** is composed of five different hydrogen-bonding fragments where "primes" denote the molecular assembly generated by inversion of original ones. Units **A**-**E** are expressed in purple, green, green, red and orange, respectively. (c) Composition of the five different hydrogen-bonding units (**A**-**E**) with dotted lines corresponding to N-H···N hydrogen bonds. Except for those involved in hydrogen bonds, hydrogen atoms are omitted for clarity.

In Fig. 1(c) are shown the five kinds of asymmetric DABCO and CH_3CN containing assemblies that comprise the one-dimensional chain in the crystal, where **A** through **E** units are $(CH_3CN\text{-}(HDABCO^+)_3)$, $(HDABCO^+\text{-}CH_3CN)$, $(CH_3CN\text{-}HDABCO^+)$, $((HDABCO^+)_2\text{-}(CH_3CN)_3)$, and $(HDABCO^+)_2(DABCO)$, respectively. Each chain is comprised of the array **A-B-C-D-E-E'-D'-C'-B'-A'** where "prime" denotes inverted members of the original molecular assembly generated. A total of 28 DABCO, CH_3CN and $(CH_3CN)_3$ components along with 18 protons are present along the more than 150 Å long *c* axis of each unit cell.

Although the positions of protons cannot be directly determined from inspection of X-ray data, all DABCO molecules in units **A**-**D** should be protonated. The N•••N distances between the hydrogen bonded nitrogen atoms of DABCO and CH_3CN are in the range of 2.856 to 3.000 Å in the **A**-**D** units (Table S1), which is fully consistent with existence of protons between the DABCO and CH_3CN nitrogens. The remaining two DABCO molecules in unit **A** are protonated and engaged in hydrogen bonds with adjacent DABCO molecules with N•••N distances of 2.863 and 2.818 Å. As a result, no protons exist between units **A** and **B** as well as between units **C** and **D**, which is consistent with the observed DABCO-DABCO N-N distances of 3.393 and 3.267 Å, respectively. Therefore, it is most likely that unit **E** is composed of $(HDABCO^+)_2(DABCO)$ units. One of the outer nitrogens of the DABCO moieties in unit **E** should be neutral so that it can interact with methyl group of CH_3CN. Finally, the DABCO molecules interacting with the two protons inside unit **E** have shorter N•••N distances than do those between units **E**.

In the crystallographic data of **1**, the DABCO molecules in units **B** and **C** as well as one in unit **E** display large thermal ellipsoids. These molecules are located in spaces between $[Ni(dmit)_2]$ layers and, thus, they experience a higher degree of motional freedom.

The $[Ni(dmit)_2]$ anions in the crystal of **1** interact in a side-by-side manner to form two-dimensional layers in the *a*-*b* plane, which are stacked along the *c* axis to produce a honeycomb like channel structure (Fig. 2(a)). Two kinds of $[Ni(dmit)_2]$ layers exist that are composed of two sets of crystallographically independent $[Ni(dmit)_2]$ anions (layers **K** and **L**, Fig. 2(b) and 2(c), respectively). These layers are stacked in a -**K**-**L**-**K**- manner along the *c* axis.

To evaluate the magnitude of the intermolecular interactions that exist between $[Ni(dmit)_2]$ anions oriented in this manner, we calculated intermolecular transfer integral (*t*, meV), which also corresponds to the magnitude of the intermolecular magnetic exchange interaction. The results show that relatively strong interactions occur within the hexamer with t_1 = + 49.91 and t_2 = – 43.91 for layer **K** and t_4 = – 47.29 for layer **L**. The two hexamers are connected with each other by interactions t_6 = + 15.72 and t_7 = + 15.72 between the layers. Inter-hexamer interactions within a layer (t_3 = – 2.29 and t_5 = + 0.02 for layer **K** and **L**, respectively) as well as those between layers **K** (t_8 = – 2.97) are small. Therefore, from the perspective of magnetic interactions, $[Ni(dmit)_2]$ anions form trimer units composed of three hexamers within the crystal of **1**.

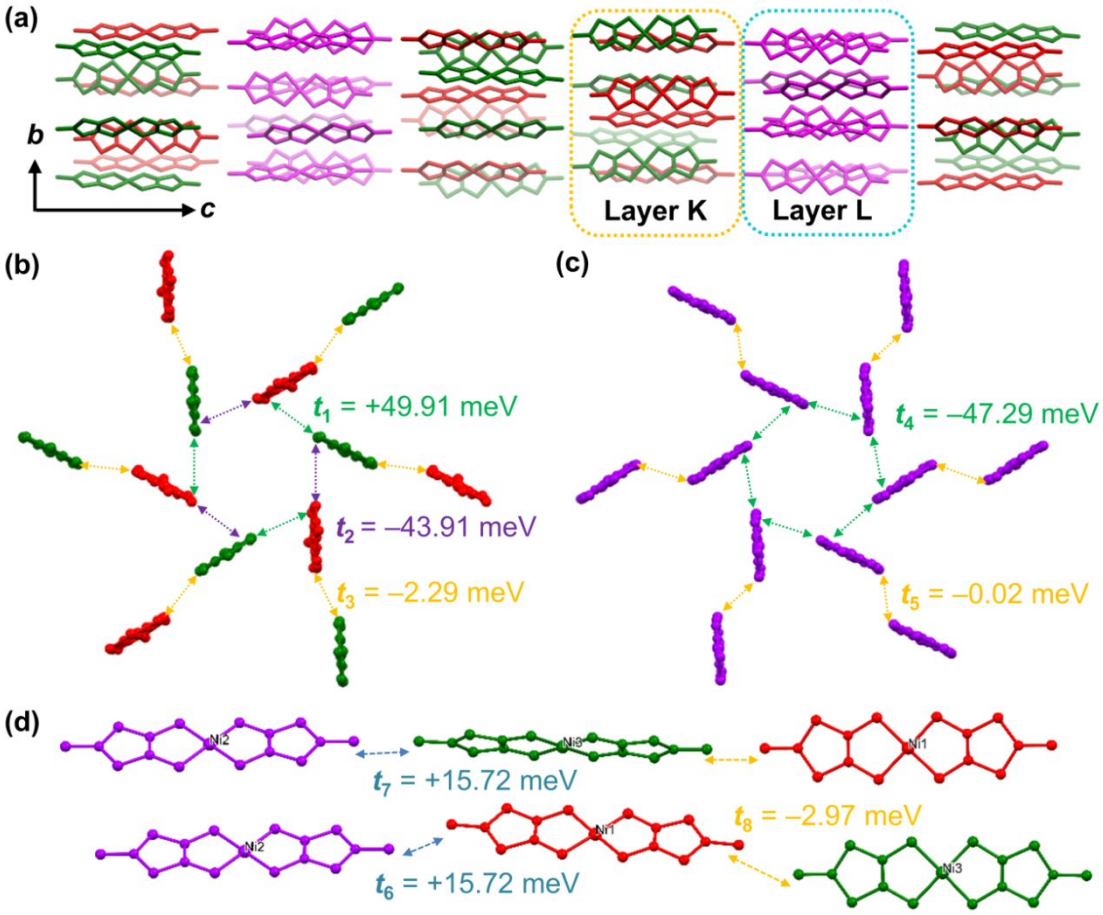

Fig. 2 (a) Arrangements of $[Ni(dmit)_2]$ anions in the crystal of **1** viewed along the *a* axis. The blue and yellow dashed boxes represent layers **K** and **L**, respectively. Layers are arranged in a (-**K**-**L**-**K**-) manner along the *c* axis. (b, c, and d) The transfer integrals in layer **K** (b) and, **L** (c), and between layers (d).

Dielectric and magnetic properties

The temperature and frequency dependence of the dielectric constant (ε_1) of a crystal **1** are shown in the plot given in Fig. 3(a). For these measurements, the electric field was applied along the direction of the one-dimensional HDABCO chain (*c*-axis). Although unlike the case of $(HDABCO^+)_2(TCNQ)_3$, the crystal of **1** does not contain a continuous hydrogen bonding chain, two kinds of relaxation phenomena occur around 100 and 300 K with respective activation energies (E_a) of 7.8 and 26.4 kJ mol^{-1}. The E_a values for DABCO rotation in several complexes were estimated based on solid-state ^{1}H-NMR spin-lattice relaxation.[33,34] The E_a for the rotation of DABCO in the crystal of 1:2 adduct with 2-chlorobenzoic acid was 22.2 kJ mol^{-1} with T_1 minimum of 210 K in the ^{1}H NMR spectrum. In the halogen-bonded molecular complex DABCO-2(iodopentafluorobenzene), two DABCO molecules are crystallographically non-equivalent and they rotate with E_a values of 20 and 11 kJ mol^{-1} with T_1 minima of 210 and 140 K in ^{1}H NMR, respectively.[34] Therefore, the observed relaxations in crystal **1** may be a consequence of molecular rotation of DABCO molecules in different crystal environments as seen in Fig. 1 (c).

The temperature dependence of the product of the molar magnetic susceptibility (χ_m) and temperature ($\chi_m T$ versus T) for a polycrystalline sample of **1** is shown in the plot given in Fig. 3(b). Inspection of the plot shows that $[Ni(dmit)_2]$ anions display antiferromagnetic interactions at higher temperatures. The values above 50 K are well fitted by using the Curie-Weiss law with a Curie constant (C) and Weiss temperature (ϑ) of 3.45 cm^3 K mol^{-1} and -58 K, respectively. Rather strong antiferromagnetic interactions exist, which correspond to intrahexamer interactions with t values around 50 meV, where the magnitude of magnetic exchange interaction (J) is proportional to the square of t.[35–37] Below 50 K, $\chi_m T$ values are larger than those expected based on the Curie-Weiss law. In

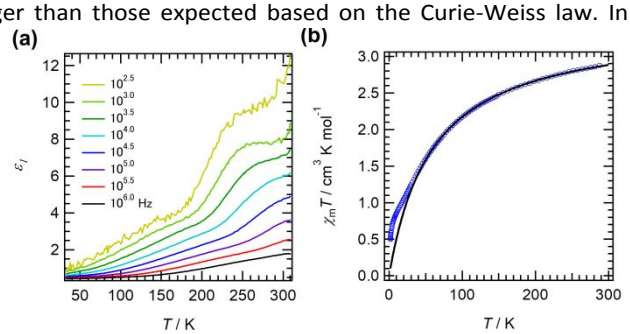

Fig. 3 (a) Temperature and frequency dependence of the dielectric constant (ε_1) measured on a single crystal of **1** along the *c* axis. (b) The $\chi_m T$ versus T plot for polycrystalline sample of **1**. Solid line indicates the fit by Curie-Weiss law above 50 K (see text).

the temperature range of 50-0 K, an abrupt decrease of $\chi_m T$ takes place as the temperature is lowered. The excess of $\chi_m T$ suggests that ferromagnetic interactions occur between hexamers within and/or between trimers composed of three hexamers. In the low temperature range, the magnetic properties are dominated by antiferromagnetic interactions in the whole crystal of **1**.

Conclusions

In the above effort, we prepared and assessed the structural and magnetic properties of the highly symmetric crystal of $(HDABCO^+)_9(DABCO)[Ni(dmit)_2]_9 \bullet 6CH_3CN$ (**1**), in which a hexagonal distribution of $[Ni(dmit)_2]$ anions creates a one-dimensional channel structure. Because the crystal of **1** does not contain a uniform DABCO chain in the channels, its dielectric response is limited to those arising from weak relaxation of molecular motion. The polymorph explored in this study contains a total of 28 DABCO, CH_3CN and $(CH_3CN)_3$ components along with 18 protons along the *c* axis of each unit cell. Considering that $HDABCO^+$ has a length along the channel of ca. 5.2 Å, an ideal crystal **1** should contain 29 DABCO units along with 18 protons in its unit cell. Such crystals might have been present among the large number of polymorphs and pseudo polymorphs of (DABCO)-$[Ni(dmit)_2]$ that can be generated. From a magnetic perspective, space groups of the crystals in trigonal crystal system such as *R*-3 are interesting as candidates for spin frustration systems.[38] Studies guided by these thoughts are in progress.

Conflicts of interest

There are no conflicts to declare.

Acknowledgements

We thank Dr. Norihisa Hoshino of IMRAM, Tohoku University, for fruitful discussions, Ms. Ai Tokumitsu of Global Facility Center, Hokkaido University for elemental analysis, and Dr. Shuhei Fukuoka and Dr. Satoaki Matsunaga of Faculty of Science, Hokkaido University for χm measurements. This study was supported financially by JSPS KAKENHI (grant. No. JP18H01949 and JP19K15517), JST-PRESTO (grant no JPMJPR19L3), JSPS Joint Research Projects under the Bilateral Programs, "Dynamic Alliance for Open Innovation Bridging Human, Environment and Materials", and Research Program of "Network Joint Research Center for Materials and Devices: Dynamic Alliance for Open Innovation Bridging Human, Environment and Materials".

Notes and references

1 G. Fischer and L. Genzel, *Zeitschrift für Phys. B Condens. Matter*, 1988, **71**, 509–514.
2 N. Yasuda, K. Sumi, H. Shimizu, S. Fujimoto and Y. Inuishi, *Jpn. J. Appl. Phys.*, 1979, **18**, 1485–1492.
3 H. M. Zeyada, N. A. El-Ghamaz and E. A. Gaml, *Phys. B Condens. Matter*, 2017, **519**, 76–81.
4 X. Hou, X. Li and H. Ye, *Polyhedron*, 2015, **102**, 657–663.
5 A. Katrusiak and M. Szafrański, *J. Am. Chem. Soc.*, 2006, **128**, 15775–15785.
6 D. Paliwoda, M. Szafrański, M. Hanfland and A. Katrusiak, *J. Mater. Chem. C*, 2018, **6**, 7689–7699.
7 S. Horiuchi, Y. Tokunaga, G. Giovannetti, S. Picozzi, H. Itoh, R. Shimano, R. Kumai and Y. Tokura, *Nature*, 2010, **463**, 789–792.
8 S. Horiuchi and S. Ishibashi, *J. Phys. Soc. Japan*, 2020, **89**, 051009.
9 A. Katrusiak and M. Szafrański, *Phys. Rev. Lett.*, 1999, **82**, 576–579.
10 S. Horiuchi, F. Kagawa, K. Hatahara, K. Kobayashi, R. Kumai, Y. Murakami and Y. Tokura, *Nat. Commun.*, 2012, **3**, 1308.
11 P. P. Shi, Y. Y. Tang, P. F. Li, W. Q. Liao, Z. X. Wang, Q. Ye and R. G. Xiong, *Chem. Soc. Rev.*, 2016, **45**, 3811–3827.
12 S. Horiuchi and Y. Tokura, *Nat. Mater.*, 2008, 7, 357–366.
13 H. Y. Ye, D. W. Fu, Y. Zhang, W. Zhang, R. G. Xiong and S. D. Huang, *J. Am. Chem. Soc.*, 2009, **131**, 42–43.
14 J. Zhang, Y. S. Wang, B. Xu and K. L. Yao, *Solid State Commun.*, 2014, **185**, 47–51.
15 S. Horiuchi, R. Kumai and Y. Tokura, *Chem. Commun.*, 2007, 2321–2329.
16 R. Kumai, S. Horiuchi, H. Sagayama, T. H. Arima, M. Watanabe, Y. Noda and Y. Tokura, *J. Am. Chem. Soc.*, 2007, **129**, 12920–12921.
17 Z. H. Wei, Z. T. Jiang, X. X. Zhang, M. L. Li, Y. Y. Tang, X. G. Chen, H. Cai and R. G. Xiong, *J. Am. Chem. Soc.*, 2020, **142**, 1995–2000.
18 Z. S. Yao, K. Yamamoto, H. L. Cai, K. Takahashi and O. Sato, *J. Am. Chem. Soc.*, 2016, **138**, 12005–12008.
19 W. Y. Zhang, Y. Y. Tang, P. F. Li, P. P. Shi, W. Q. Liao, D. W. Fu, H. Y. Ye, Y. Zhang and R. G. Xiong, *J. Am. Chem. Soc.*, 2017, **139**, 10897–10902.
20 M. Szafrański, *J. Phys. Chem. B*, 2009, **113**, 9479–9488.
21 M. Szafrański, A. Katrusiak and G. J. McIntyre, *Phys. Rev. Lett.*, 2002, **89**, 3–6.
22 T. Akutagawa, S. Takeda, T. Hasegawa and T. Nakamura, *J. Am. Chem. Soc.*, 2004, **126**, 291–294.
23 P. Cassoux, L. Valade, H. Kobayashi, A. Kobayashi, R. A. Clark and A. E. Underhill, *Coord. Chem. Rev.*, 1991, **110**, 115–160.
24 P. Cassoux, *Coord. Chem. Rev.*, 1999, **185**, 213–232.
25 G. Liu, Q. Fang and C. Wang, *J. Mol. Struct. THEOCHEM*, 2004, **679**, 115–120.
26 G. Steimecke, H.-J. Sieler, R. Kirmse and E. Hoyer, *Phosphorous Sulfur Relat. Elem.*, 1979, **7**, 49–55.
27 G. M. Sheldrick, *Acta Crystallogr. Sect. A Found. Adv.*, 2015, **71**, 3–8.
28 O. V Dolomanov, L. J. Bourhis, R. J. Gildea, J. A. K. Howard and H. Puschmann, *J. Appl. Crystallogr.*, 2009, **42**, 339–341.
29 G. A. Bain and J. F. Berry, *J. Chem. Educ.*, 2008, **85**, 532–536.
30 T. Mori, A. Kobayashi, Y. Sasaki, H. Kobayashi, G. Saito and H. Inokuchi, *Bull. Chem. Soc. Jpn.*, 1984, **57**, 627–633.

31 T. Imakubo, T. Maruyama, H. Sawa and K. Kobayashi, *Chem. Commun.*, 1998, 2021–2022.
32 N. Kobayashi, T. Naito and T. Inabe, *Adv. Mater.*, 2004, **16**, 1803–1806.
33 T. Asaji, *J. Mol. Struct.*, 2018, **1159**, 174–178.
34 T. Asaji, K. Shido and H. Fujimori, *J. Mol. Struct.*, 2018, **1169**, 81–84.
35 J. C. Scott, *Semiconductors and Semimetals: Highly Conducting Quasi One-dimensional Organic Crystals*, Academic Press, San Diego, 1988.
36 T. Akutagawa, T. Nakamura, T. Inabe and A. E. Underhill, *Thin Solid Films*, 1998, **331**, 264–271.
37 T. Akutagawa and T. Nakamura, *Coord. Chem. Rev.*, 2002, **226**, 3–9.
38 L. Postulka, S. M. Winter, A. G. Mihailov, A. Mailman, A. Assoud, C. M. Robertson, B. Wolf, M. Lang and R. T. Oakley, *J. Am. Chem. Soc.*, 2016, **138**, 10738–10741.

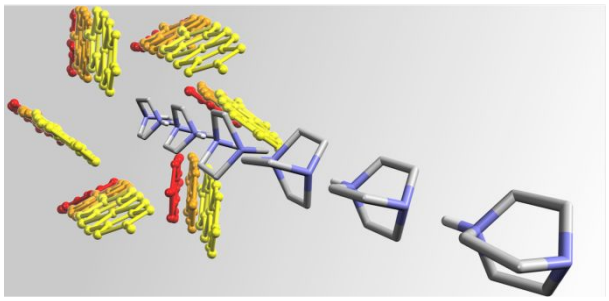

$(HDABCO^{+})_9(DABCO)[Ni(dmit)_2]_9 \bullet 6CH_3CN$ had a hexapetal flower-like pattern of $[Ni(dmit)_2]^{-}$. The $[Ni(dmit)_2]^{-}$ hexamers formed trimer units and stacked one-dimensionally including DABCO-CH_3CN chain at the centre more than 150 Å long per unit cell.